

# Frequency-dependent mitochondrial $\text{Ca}^{2+}$ accumulation regulates ATP synthesis in pancreatic $\beta$ cells

Andrei I. Tarasov · Francesca Semplici · Daliang Li ·  
Rosario Rizzuto · Magalie A. Ravier · Patrick Gilon ·  
Guy A. Rutter

Received: 28 September 2012 / Revised: 25 October 2012 / Accepted: 29 October 2012 / Published online: 14 November 2012  
© The Author(s) 2012. This article is published with open access at Springerlink.com

**Abstract** Pancreatic  $\beta$  cells respond to increases in glucose concentration with enhanced metabolism, the closure of ATP-sensitive  $\text{K}^+$  channels and electrical spiking. The latter results in oscillatory  $\text{Ca}^{2+}$  influx through voltage-gated  $\text{Ca}^{2+}$  channels and the activation of insulin release. The relationship between changes in cytosolic and mitochondrial free calcium concentration ( $[\text{Ca}^{2+}]_{\text{cyt}}$  and  $[\text{Ca}^{2+}]_{\text{mit}}$ , respectively) during these cycles is poorly understood. Importantly, the activation of  $\text{Ca}^{2+}$ -sensitive intramitochondrial dehydrogenases, occurring alongside the stimulation of ATP consumption required for  $\text{Ca}^{2+}$  pumping and other processes, may exert complex effects on cytosolic ATP/ADP ratios and

hence insulin secretion. To explore the relationship between these parameters in single primary  $\beta$  cells, we have deployed cytosolic (Fura red, Indo1) or green fluorescent protein-based recombinant-targeted (*Pericam*, 2mt8RP for mitochondria; D4ER for the ER) probes for  $\text{Ca}^{2+}$  and cytosolic ATP/ADP (*Perceval*) alongside patch-clamp electrophysiology. We demonstrate that: (1) blockade of mitochondrial  $\text{Ca}^{2+}$  uptake by shRNA-mediated silencing of the uniporter MCU attenuates glucose- and essentially blocks tolbutamide-stimulated, insulin secretion; (2) during electrical stimulation, mitochondria decode cytosolic  $\text{Ca}^{2+}$  oscillation frequency as stable increases in  $[\text{Ca}^{2+}]_{\text{mit}}$  and cytosolic ATP/ADP; (3) mitochondrial  $\text{Ca}^{2+}$  uptake rates remained constant between individual spikes, arguing against activity-dependent regulation (“plasticity”) and (4) the relationship between  $[\text{Ca}^{2+}]_{\text{cyt}}$  and  $[\text{Ca}^{2+}]_{\text{mit}}$  is essentially unaffected by changes in endoplasmic reticulum  $\text{Ca}^{2+}$  ( $[\text{Ca}^{2+}]_{\text{ER}}$ ). Our findings thus highlight new aspects of  $\text{Ca}^{2+}$  signalling in  $\beta$  cells of relevance to the actions of both glucose and sulphonylureas.

**Electronic supplementary material** The online version of this article (doi:10.1007/s00424-012-1177-9) contains supplementary material, which is available to authorized users.

A. I. Tarasov · F. Semplici · G. A. Rutter (✉)  
Section of Cell Biology, Division of Diabetes Endocrinology and Metabolism, Department of Medicine, Imperial College London, SW7 2AZ London, UK  
e-mail: g.rutter@imperial.ac.uk

D. Li  
Department of Cell Biology and of Biochemistry, University of Texas Southwestern Medical Center,  
Dallas, TX 75390-9039, USA

R. Rizzuto  
Department of Biomedical Sciences, University of Padua,  
35121 Padua, Italy

M. A. Ravier  
Institut de Génomique Fonctionnelle, INSERM U661, CNRS UMR5203, Université Montpellier I et II,  
34094 Montpellier Cedex 5, France

P. Gilon  
diabète et nutrition, Pôle d’endocrinologie, Institut de recherche expérimentale et clinique, Université catholique de Louvain,  
Brussels, Belgium

**Keywords** Insulin secretion · Calcium · Oscillation · Mitochondria · MCU · ATP

## Abbreviations

$[\text{ATP/ADP}]_{\text{cyt}}$	Apparent free cytosolic ATP/ADP ratio
$[\text{Ca}^{2+}]_{\text{cyt}}$ , $[\text{Ca}^{2+}]_{\text{mit}}$ , $[\text{Ca}^{2+}]_{\text{ER}}$	Mitochondrial and endoplasmic reticulum free $\text{Ca}^{2+}$ concentrations, respectively
ER	Endoplasmic reticulum
FCCP	Carbonyl cyanide 4-(trifluoromethoxy)phenylhydrazone
$G_m$	Whole-cell conductance
$I_m$	Whole-cell current
IP3	Inositol 1,4,5-trisphosphate

$K_{ATP}$	ATP-sensitive $K^+$ channels
MCU	Mitochondrial calcium uniporter
NCLX	Sodium-calcium (lithium) exchanger
ROI	Region of interest
T2D	Type 2 diabetes
$V_m$	Plasma membrane electrical potential

## Introduction

A wide range of extracellular stimuli, including receptor agonists and nutrients, trigger cytosolic  $Ca^{2+}$  oscillations as a means of transmitting a signal to the cell interior [7]. These  $Ca^{2+}$  rises are decoded by calcium binding proteins which ultimately regulate key functions such as energy metabolism [1, 12], growth and development [54], activation [15] and apoptosis [37]. Pulsatile  $Ca^{2+}$  changes are thus important both (a) to provide the opportunity for intricate spatiotemporal control of intracellular events [48] and (b) to avoid the need for a sustained calcium rise, which may provoke undesirable effects such as the formation of insoluble calcium complexes and potentially catastrophic structural damage. At present, however, the machinery which distinguishes pulsatile  $Ca^{2+}$  rises from a sustained increase of the same amplitude is only partly defined [15].

Glucose induces the secretion of insulin from the pancreatic  $\beta$  cell through the stimulation of oxidative metabolism, an elevation in cytosolic ATP/ADP ratios and the closure of ATP-sensitive  $K^+$  channels ( $K_{ATP}$ ). The subsequent depolarisation of the plasma membrane then leads to bursting electrical activity, the influx of  $Ca^{2+}$  through voltage-gated  $Ca^{2+}$  channels and the activation of secretory granule exocytosis [44, 55]. In addition, further mechanisms, independent of  $K_{ATP}$  channels, amplify the effects of  $Ca^{2+}$  [23]. Mitochondrial metabolism is particularly important in the triggering of insulin secretion [30], with >95 % of glucose-derived carbon atoms being oxidised within these organelles [50, 55] in a process further stimulated by activation of the glycerol phosphate shunt by  $[Ca^{2+}]_{cyt}$  [45]. Increases in mitochondrial free calcium ( $[Ca^{2+}]_{mit}$ ) in response to glucose [1, 25] or other stimuli [47] have also been suggested to activate intramitochondrial dehydrogenases [12, 42]. These events are together likely to stimulate mitochondrial ATP synthesis, providing a positive feedback mechanism to further enhance insulin secretion [43].

We have recently developed an approach to monitoring intracellular free  $Ca^{2+}$  in multiple compartments simultaneously in the same living cell, whilst measuring (or manipulating) membrane potential through the patch pipette [51, 53]. Thus, the mitochondrial matrix-targeted  $Ca^{2+}$  sensitive

probe, *pericam*, is used alongside an intracellularly trap-pable calcium probe, Fura red [52], to monitor changes in mitochondrial and cytosolic free  $Ca^{2+}$ , respectively [51]. Likewise, the ATP-sensitive probe *Perceval* [6] can be used to monitor changes in cytosolic ATP/ADP ratio simultaneously with cytosolic  $Ca^{2+}$  [51]. In this way, we have demonstrated [53] that glucose-induced increases in intramitochondrial free  $Ca^{2+}$ , mediated by the mitochondrial uniporter (MCU) [5, 11] and modulated by the  $Na^+$ - $Ca^{2+}$  exchanger NCLX, are required for normal increases in cytosolic ATP/ADP ratio. On the other hand, neither the relationship between  $[Ca^{2+}]_{cyt}$  and  $[Ca^{2+}]_{mit}$  during temporally complex changes in the former nor the relationship between cytosolic  $Ca^{2+}$  and  $Ca^{2+}$  in other organelles, e.g. the endoplasmic reticulum, was explored.

An interesting finding made during our earlier studies [53] was that increases and decreases in intramitochondrial  $Ca^{2+}$  are significantly delayed with respect to those in the cytosol when these are changed in a single step. This has raised the question as to how mitochondrial  $Ca^{2+}$  may respond to repetitive, oscillatory changes in cytosolic  $Ca^{2+}$ . This issue is of particular physiological importance since both glucose-induced cytosolic  $Ca^{2+}$  increases [47] and insulin secretion [34] are pulsatile in nature, a feature that may be driven by glycolytic oscillations [8] and the complex interplay of ion channel activities [32] which lead to bursts in electrical activity. Whether oscillatory changes in mitochondrial  $Ca^{2+}$ , and hence pulses in ATP synthesis, can then occur and may contribute to the control of insulin secretion has yet to be determined [2, 13].

We therefore sought here to determine how oscillations in electrical activity, and hence cytosolic  $Ca^{2+}$ , are decoded by  $\beta$  cell mitochondria in situ. We also examined the impact of cytosolic  $[Ca^{2+}]$  oscillations on the concentration of this ion within the endoplasmic reticulum and assessed whether fluxes between the  $Ca^{2+}$  and the ER may influence  $[Ca^{2+}]_{mit}$  dynamics.

We show that attenuation of  $[Ca^{2+}]_{mit}$  increases, achieved by silencing MCU, inhibits insulin secretion, demonstrating the importance of mitochondrial calcium accumulation for the normal regulation of hormone release from primary  $\beta$  cells. We then demonstrate that the *amplitude* of the  $[Ca^{2+}]_{mit}$  increases displays a remarkable dependence upon the *frequency* of  $[Ca^{2+}]_{cyt}$  oscillations. Thus, “frequency-amplitude decoding” of the oscillations by mitochondria allows the modulation of ATP/ADP production whilst bypassing the need for stable, and potentially damaging, increases in  $[Ca^{2+}]_{cyt}$ .

## Materials and methods

### Islet isolation and culture

Female CD1 mice (10–12 weeks of age) were obtained from Charles Rivers (Margate, UK) and fed ad libitum prior to

use. After cervical dislocation according to UK Home Office approved procedures (Animals Scientific Procedures Act, 1986), pancreatic islets were isolated by infusion of collagenase via the pancreatic duct [41]. After pre-culture for 5 h in RMPI-1640 medium, containing 11 mM glucose, 10 % FCS, 100  $\mu$ U penicillin, 100  $\mu$ g streptomycin, at 37 °C, 5 % CO<sub>2</sub>, in absolute humidity, islets were infected with adenoviruses delivering the cDNA encoding the required probe, split into single  $\beta$  cells by mechanical disruption and plated on glass coverslips. Cells were then cultured for a further >24 h for 2–5 days and assayed as described below. Glass-attached single cells or two- to three-cell clusters displayed an infection efficiency of >90 % [41].

### Molecular biology and generation of adenoviruses

Adenoviruses encoding the ATP/ADP sensor Perceval [6] or the mitochondrial Ca<sup>2+</sup> sensor 2mt8-ratiometric pericam (2mt8RP) [18] were generated as described [51]. MCU was silenced using a suitable lentivirus (Santa Cruz) as described [53] and verified by qRT-PCR.

To measure [Ca<sup>2+</sup>]<sub>ER</sub>, an adenovirus encoding D4ER was used [40]. This construct includes cDNA encoding D1ER [35], modified by replacing the Ca<sup>2+</sup> binding domain D1 with the low affinity Ca<sup>2+</sup> sensor D4, downstream of the rat insulin promoter. Recombination with pAdEasy-1, transfection into HEK293 cells and adenoviral particle production were achieved according to published protocols [28].

### Single cell epifluorescence imaging

Simultaneous imaging of free [Ca<sup>2+</sup>] in mitochondria and in the cytosol was performed essentially as described [51] using the mitochondrial pericam 2mt8RP and Fura-Red (Invitrogen), respectively; [Ca<sup>2+</sup>] was measured simultaneously in the ER and cytosol using D4ER cameleon and Indo-1 (Invitrogen). 2mt8RP, Fura-Red and Indo-1 were examined at single excitation and emission wavelengths. Either dye was dissolved in DMSO (4 mM) containing 4 % F127-Pluronic. Cells were loaded by incubation with either dye (4  $\mu$ M) in the extracellular solution for 30 min. Imaging experiments were performed on an Olympus IX-71 microscope with a UPlanFL N $\times$ 40, NA 1.2 objective. For acquisition, an F-View-II camera and MT-20 excitation system equipped with a Hg/Xe arc lamp were used, under control of Cell'R software (Olympus). The excitation/emission wavelengths were (nanometres): 410 of 535 (2mt8RP), 490 of 630 (Fura-Red), 490 of 535 (perceval), 440 of (465 and 530) (D4ER cameleon) and 350 of 465 (Indo-1). In all cases, cells were maintained at 3 mM glucose for 15–30 min prior to stimulation at the indicated glucose concentrations. Images were acquired at a frequency of 0.2 Hz (apart from Fig. 2a, where a frequency of 2 Hz was used). Every Ca<sup>2+</sup>

recording was subjected to the dynamic range control by applying, at the end of the trace, solutions containing 10  $\mu$ M ionomycin: “Ca<sup>2+</sup>-free” (0.5 mM EGTA) and “Ca<sup>2+</sup>-max” (5 mM Ca<sup>2+</sup>). The acquisition of the fluorescence and electrophysiological data was synchronized using TTL pulse.

Imaging data were background-subtracted, analysed and presented as  $F/F_0$  (perceval),  $R/R_0$  530/465 (D4ER) and  $F_0/F$  (Fura-Red, Indo-1, 2mt8RP). Whole cells were selected as regions of interest (ROI) to minimize the drift effects during the long recordings. In the case of a cell cluster, only the cell that was patched was included in the ROI. Changes in the fluorescence of zinc indicator for measuring induced exocytosis of zinc (ZIMIR) were measured as previously described [26]. The properties of the FRET probes used here are described in previous publications [6, 40, 53].

### Electrophysiology

Electrophysiological recordings and stimulation were done in the whole-cell perforated-patch configuration, using an EPC9 patch-clamp amplifier controlled by Pulse acquisition software (HEKA Elektronik). The pipette tip was dipped into pipette solution and then back-filled with the same solution containing 0.17  $\mu$ g/ml amphotericin B. Series resistance and cell capacitance were compensated automatically by the acquisition software. Recordings, triggered by the TTL pulse, were started in current-clamp mode, and the depolarization of the plasma membrane was monitored simultaneously with [Ca<sup>2+</sup>] and [ATP/ADP]<sub>cyt</sub>, in response to a glucose step from 3 to 10 or 16.7 mM. After the onset of electrical activity, the mode was switched to voltage clamp to control  $V_m$  and impose electrical stimulations.  $V_m$  was held at the value of  $-70$  mV. Electrical stimulation was imposed to mimic the naturally occurring bursts of action potentials and comprised 5-s depolarization trains to  $-30$  mV containing 25 ramps of 100+100 ms to 0 mV and back (Suppl. Fig. S1). The artificial bursts were applied at different frequencies: every 10, 4, 2, 1 and 0.5 min<sup>-1</sup>, which correspond to “duty cycle” values of 0.9, 0.36, 0.18, 0.09 and 0.045, respectively. Data were filtered at 1 kHz and digitised at 2 kHz.

### Experimental solutions

The pipette solution contained (millimolar): 76 K<sub>2</sub>SO<sub>4</sub>, 10 NaCl, 10 KCl, 1 MgCl<sub>2</sub>, 5 HEPES (pH 7.35 with KOH). The extracellular bath solution, referred in text as “EC” contained (millimolar): 120 NaCl, 4.8 KCl, 24 NaHCO<sub>3</sub> (saturated with CO<sub>2</sub>), 5 HEPES (pH 7.4 with NaOH), 2.5 CaCl<sub>2</sub>, 1.2 MgCl<sub>2</sub>. All experiments were conducted at 32–33 °C, and the bath solution was perfused continuously.

## Data analysis

Imaging data were analysed using Cell<sup>^</sup>R (Olympus), ImageJ (Wayne Rasband, NIMH) and MS Excel. Simultaneous recordings were combined and analysed using Igor Pro (Wavemetrics). The results are presented as mean  $\pm$  SEM. A Mann–Whitney *U* test was used to assess the statistical significance of the differences between the independent samples. Wilcoxon's paired test was used in case of dependent samples. The significance values are specified in each figure; as a rule,  $p < 0.05$  differences were considered significant.

## Results

### Mitochondrial $\text{Ca}^{2+}$ accumulation mediated by MCU modulates insulin secretion from primary mouse $\beta$ cells

Having recently reported that  $\text{Ca}^{2+}$  uptake by mitochondria is essential for glucose-stimulated ATP increases in pancreatic  $\beta$  cells [53], we sought firstly to determine whether MCU-mediated mitochondrial  $\text{Ca}^{2+}$  uptake was required for the stimulation of insulin secretion in this system. To this end, we used monolayer cultures of dispersed mouse islets, comprising single cells or small clusters of two to three cells [41]. In this preparation, MCU expression could readily be decreased by  $\sim 80\%$  through lentivirus-mediated delivery of a short hairpin RNA (shRNA; see “Materials and methods”) [53].

To assay insulin secretion from *single* cells, we used a fluorescent cell surface-attached dye, ZIMIR, which detects  $\text{Zn}^{2+}$  co-secreted with insulin [26]. In this assay, changes in ZIMIR fluorescence reflect the balance between the release of  $\text{Zn}^{2+}$  from the  $\beta$  cells and chelation of the released  $\text{Zn}^{2+}$  by low concentrations of EGTA, present in extracellular buffer. Thus, the ZIMIR signal indicates the *rate* of secretion rather than the absolute amount of secreted insulin.

Silencing of MCU led to a delay in glucose-induced ZIMIR increases (Fig. 1a–c), consistent with an inhibition of insulin secretion [26], although the amplitude of the final increase was unchanged in MCU-depleted cells. Strikingly, the effects of further stimulation with the sulphonylurea tolbutamide were substantially decreased in MCU-depleted cells (Fig. 1a, c). Sulphonylureas, which are first-choice drugs for treatment of type 2 diabetes mellitus, specifically inhibit  $\beta$  cell  $\text{K}_{\text{ATP}}$  channels, depolarise the plasma membrane and induce electrical activity even at low glucose [4]. At high glucose, when the  $\beta$  cell is already electrically active, addition of sulphonylurea is known to result in a substantial increase in the frequency of electrical spiking [17] (and data not shown). The above data (Fig. 1a, c) thus suggest that the ability of this additional excitation to

stimulate exocytosis relies upon  $\text{Ca}^{2+}$  entry into mitochondria. This prompted us to explore how electrical spikes, inducing cytosolic  $\text{Ca}^{2+}$  increases, are linked to  $\text{Ca}^{2+}$  increases in mitochondria and to the consequent increase in ATP generation by these organelles.

### Dynamics of $\beta$ cell $[\text{Ca}^{2+}]_{\text{cyt}}$ and $[\text{Ca}^{2+}]_{\text{mit}}$ during glucose-induced electrical activity

In cells in which electrical activity was stimulated by the presence of 16.7 mM glucose, Fura-Red and 2mt8RP were used to report the  $\text{Ca}^{2+}$  signals from the cytosol and mitochondrial lumen, respectively, whilst plasma membrane potential ( $V_m$ ) was measured simultaneously using the perforated patch configuration. Remarkably, the majority of individual electrical spikes prompted by glucose at  $1.1 \pm 0.1$  Hz ( $n = 37$  cells) were reliably tracked by increases and decreases in  $[\text{Ca}^{2+}]_{\text{cyt}}$  whilst  $[\text{Ca}^{2+}]_{\text{mit}}$  was increased only after a much longer lag (Fig. 2a). Indeed, increases in  $[\text{Ca}^{2+}]_{\text{mit}}$  were difficult to resolve at each peak (Fig. 2a) though the progressive elevation of  $[\text{Ca}^{2+}]_{\text{mit}}$  observed suggested that they may occur, but reverse slowly.

We next asked how  $[\text{Ca}^{2+}]_{\text{mit}}$  might respond to more widely spaced oscillations in electrical activity and  $[\text{Ca}^{2+}]_{\text{cyt}}$ , induced by an intermediate concentration of glucose. At 10 mM glucose,  $V_m$  typically displayed periodic bursting activity [33], with frequencies of one burst every 3–4 min ( $215 \pm 33$  s;  $n = 6$  cells from three separate preparations; Fig. 2b). The onset of each burst was quickly followed by an elevation in  $[\text{Ca}^{2+}]_{\text{cyt}}$ , reaching a maximum value in 10–20 s, whilst  $[\text{Ca}^{2+}]_{\text{mit}}$  increased more slowly, taking  $\sim 1$  min to plateau. The termination of each electrical burst was accompanied by a rapid relaxation of  $[\text{Ca}^{2+}]_{\text{cyt}}$  to basal levels whilst  $[\text{Ca}^{2+}]_{\text{mit}}$  remained significantly elevated for 1–2 min, barely falling before the onset of the next burst (Fig. 2b). Thus, mitochondria discriminate between continuous spiking (every 1.5 s) and slow bursting (every 215 s) induced by glucose. In the former case, mitochondria display continuously elevated  $\text{Ca}^{2+}$  whilst in the latter case  $[\text{Ca}^{2+}]_{\text{mit}}$  tracks changes in  $V_m$  and  $[\text{Ca}^{2+}]_{\text{cyt}}$ .

The amplitude of  $[\text{Ca}^{2+}]_{\text{mit}}$  increases depends on the frequency of electrically imposed  $[\text{Ca}^{2+}]_{\text{cyt}}$  oscillations

The above observations suggested that the degree of  $\text{Ca}^{2+}$  accumulation by mitochondria, and thus the *amplitude* of the observed  $[\text{Ca}^{2+}]_{\text{mit}}$  increases, may depend on the *frequency* of  $V_m$  bursts and hence  $[\text{Ca}^{2+}]_{\text{cyt}}$  increases. Thus, lower frequency pulses in  $[\text{Ca}^{2+}]_{\text{cyt}}$  might be expected to allow  $[\text{Ca}^{2+}]_{\text{mit}}$  to return to basal levels before the next spike, whereas higher-frequency pulses might allow the accumulation of  $\text{Ca}^{2+}$  by mitochondria and hence progressive increases in  $[\text{Ca}^{2+}]_{\text{mit}}$  (“summation”).



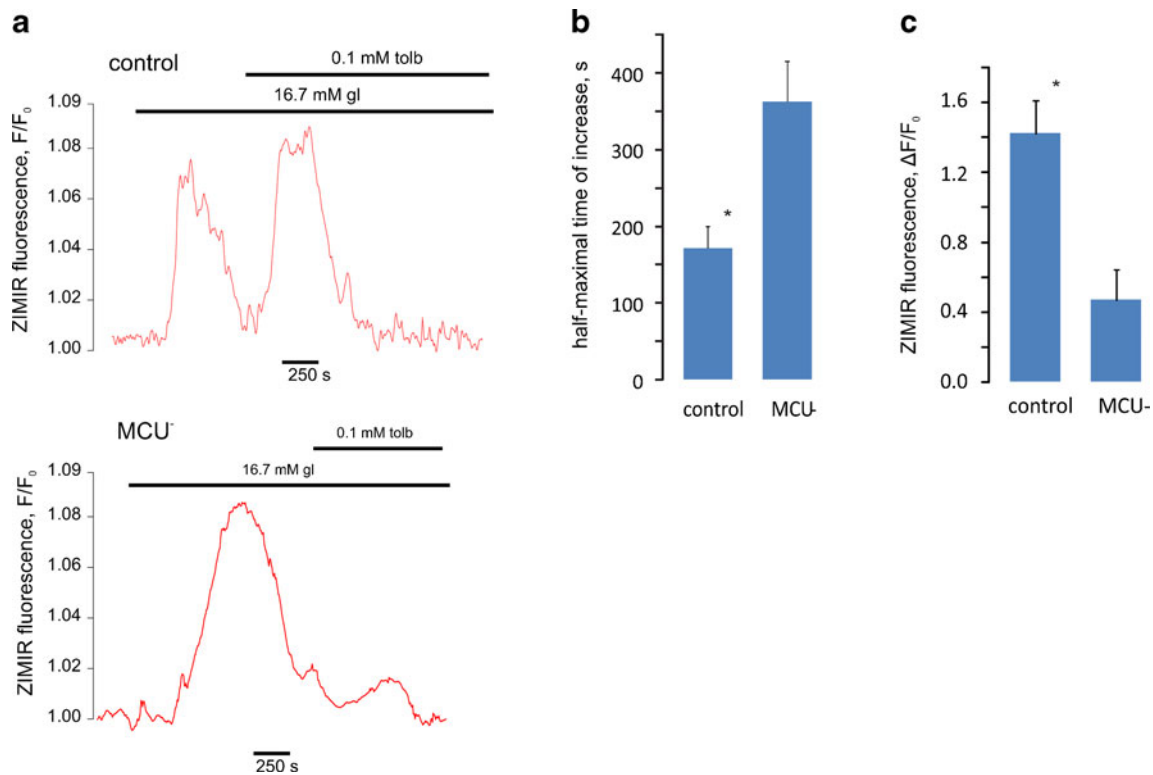


**Fig. 1** The mitochondrial  $\text{Ca}^{2+}$  uniporter MCU is required for the stimulation of insulin secretion from primary  $\beta$  cells by glucose and sulphonylureas. **a** As a surrogate for insulin secretion, the release of  $\text{Zn}^{2+}$  was imaged using ZIMIR in single  $\beta$  cells. The cells were infected with lentivirus encoding for non-sense or anti-MCU shRNA, as indicated. Cells were exposed to high glucose as

shown, after which the sulphonylurea tolbutamide was added. **b** Half-maximal times of the increase in ZIMIR fluorescence induced by 16.7 mM glucose. **c** Effect of MCU silencing on the amplitude of tolbutamide-induced increases in ZIMIR fluorescence. \* $P < 0.05$ , differences are statistically significant

In practice,  $[\text{Ca}^{2+}]_{\text{cyt}}$  changes of a specific frequency cannot readily (i.e. reproducibly between different single  $\beta$  cells) be imposed through the modulation of glucose concentrations alone. Moreover, step increases in glucose concentration would in any case be expected to enhance glycolytic and oxidative metabolism through a substrate supply effect. This, in turn, should increase respiratory chain activity and mitochondrial ATP synthesis independently of any action of  $\text{Ca}^{2+}$  on intramitochondrial metabolism. To avoid these confounding effects, we therefore imposed  $[\text{Ca}^{2+}]_{\text{cyt}}$  oscillations of varying frequency by manipulating the plasma membrane potential, and hence the activity of voltage-gated  $\text{Ca}^{2+}$  channels, using voltage clamp.

We thus applied depolarisations of constant amplitude (Fig. S1A) but varying frequency (1–10  $\text{min}^{-1}$ ; Fig. 3a, b). The parameters of the stimulation protocol were chosen to mimic the electrical activity that occurs naturally in intact islets [20]. Examined at 16.7 mM glucose, stimulation at each of the frequencies tested caused clear and large increases in  $[\text{Ca}^{2+}]_{\text{cyt}}$ , reflecting influx across the plasma membrane (Fig. 3a, b). Indeed, the amplitude of the  $[\text{Ca}^{2+}]_{\text{cyt}}$  increases was essentially maximal even at the lowest frequency tested (1.0  $\text{min}^{-1}$ ;

Fig. 3b). By contrast, the amplitude of the corresponding  $[\text{Ca}^{2+}]_{\text{mit}}$  peaks increased progressively with depolarisation frequency, effectively doubling between 1 and 2  $\text{min}^{-1}$  and again between 2 and 10  $\text{min}^{-1}$  (Fig. 3b). The relationship between burst frequency, and the mean amplitude of the  $[\text{Ca}^{2+}]_{\text{cyt}}$  and  $[\text{Ca}^{2+}]_{\text{mit}}$  changes, is shown in Fig. 3c. This analysis revealed a marked right-shift in the response to burst frequency of  $[\text{Ca}^{2+}]_{\text{mit}}$  when compared to  $[\text{Ca}^{2+}]_{\text{cyt}}$ . For example, in the case of  $[\text{Ca}^{2+}]_{\text{mit}}$ , ~4 bursts  $\text{min}^{-1}$  were required to achieve 80 %  $F/F_{\text{max}}$ . By contrast, the same  $F/F_{\text{max}}$  was obtained for  $[\text{Ca}^{2+}]_{\text{cyt}}$  with a burst frequency of just  $\leq 1 \text{ min}^{-1}$ .

In order to confirm the physiological validity of the stimulation protocol chosen above, we also monitored the values of  $[\text{Ca}^{2+}]_{\text{cyt}}$ ,  $[\text{Ca}^{2+}]_{\text{mit}}$  and  $V_m$  during the application of natural stimulus, high glucose (16.7 mM), alone (Fig. S1B). Subsequent voltage clamping of the same cell then allowed us to impose depolarisations at frequencies (five bursts at 4  $\text{min}^{-1}$  for the cell shown in Fig. S1) which closely replicated the changes of  $[\text{Ca}^{2+}]_{\text{cyt}}$  and  $[\text{Ca}^{2+}]_{\text{mit}}$  during the prior exposure to elevated glucose. Importantly, the frequency of bursts required to mimic stimulation with glucose typically lay mid-range in the

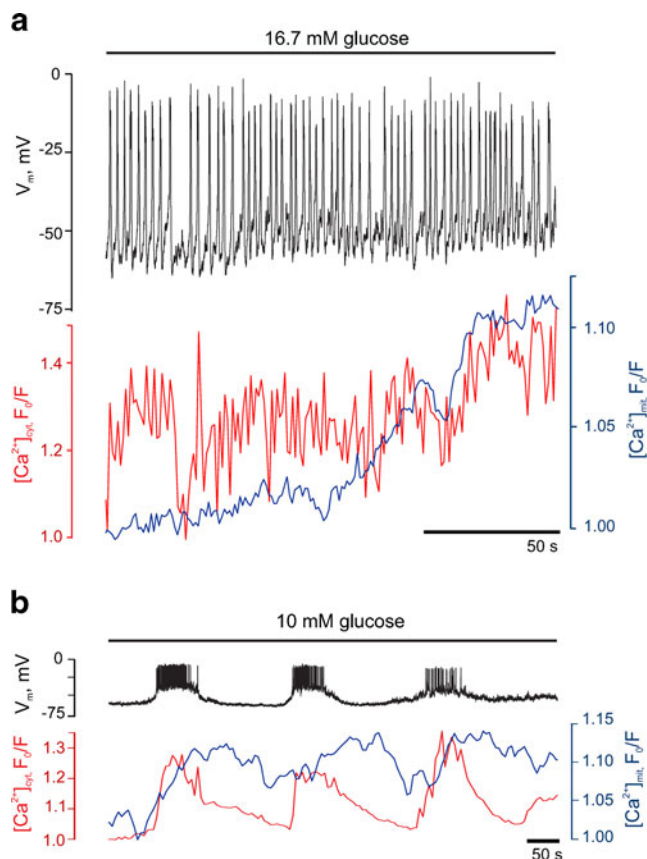


**Fig. 2** Glucose-induced cytosolic  $\text{Ca}^{2+}$  oscillations are followed by damped increases in mitochondrial free  $\text{Ca}^{2+}$  in primary  $\beta$  cells. **a** Regenerative electrical activity (black) at 16.7 mM glucose and corresponding changes in  $[\text{Ca}^{2+}]_{\text{cyt}}$  (red) and  $[\text{Ca}^{2+}]_{\text{mit}}$  (blue). **b** Representative trace of changes in electrical activity (upper trace, black),  $[\text{Ca}^{2+}]_{\text{cyt}}$  (red) and  $[\text{Ca}^{2+}]_{\text{mit}}$  (blue) induced by 10 mM glucose in a separate single  $\beta$  cell. The results are representative of at least ten further trials from different preparations

plot of burst frequency vs.  $[\text{Ca}^{2+}]_{\text{cyt}}$  and  $[\text{Ca}^{2+}]_{\text{mit}}$  shown in Fig. 3c (open squares).

Similar data to those above were obtained at 10 mM glucose (Fig. S2), whereas recordings at lower (3 mM) glucose led to a deterioration in the  $\text{Ca}^{2+}$  changes in both compartments (not shown), consistent with a requirement for sustained elevation in glucose metabolism and ATP synthesis for intracellular  $\text{Ca}^{2+}$  homeostasis during the above protocols.

“Summation” of cytosolic  $\text{Ca}^{2+}$  oscillations by mitochondria

To probe further the properties of the frequency-sensing mechanisms of mitochondria, we analysed in detail the response of  $[\text{Ca}^{2+}]_{\text{mit}}$  to stimulation by depolarising trains of different frequencies. The contribution of the each  $[\text{Ca}^{2+}]_{\text{mit}}$  peak to the maximum  $[\text{Ca}^{2+}]_{\text{mit}}$  amplitude achieved after the firing of five bursts (Fig. 4a) was quantified. This analysis revealed that the fraction of the maximal  $[\text{Ca}^{2+}]_{\text{mit}}$  reached after the first

burst progressively decreased with burst frequency (Fig. 4b). Thus, at a low burst frequency ( $2 \text{ min}^{-1}$ ), the increase in  $[\text{Ca}^{2+}]_{\text{mit}}$  provoked by the first burst represented  $\sim 70\%$  of maximum. By contrast, at the highest frequency tested ( $10 \text{ min}^{-1}$ ), the first burst achieved  $\sim 30\%$  of the maximum  $[\text{Ca}^{2+}]_{\text{mit}}$  increase. The values at intermediate burst frequencies lay between these extremes. Thus, the magnitude of the final  $[\text{Ca}^{2+}]_{\text{mit}}$  increase was dependent on the summation of individual  $[\text{Ca}^{2+}]$  increases that failed to relax to the baseline between depolarisation bursts.

Role of the endoplasmic reticulum in the interplay between  $[\text{Ca}^{2+}]_{\text{cyt}}$  and  $[\text{Ca}^{2+}]_{\text{mit}}$

We next asked whether the kinetics of the increases in  $\text{Ca}^{2+}$  in the ER may show a similar dependence on  $[\text{Ca}^{2+}]_{\text{cyt}}$  oscillation frequency to those for the mitochondrial changes measured above. ER  $\text{Ca}^{2+}$  ( $[\text{Ca}^{2+}]_{\text{ER}}$ ) was therefore measured using the probe D4ER [40] (Fig. S3), whilst cytosolic  $\text{Ca}^{2+}$  was imaged using Indo-1. During the same depolarisation protocols as used above, ER free  $\text{Ca}^{2+}$  changes were also dependent on pulse frequency (Fig. 5a vs. Fig. 3b, c). However, ER sequestered  $\text{Ca}^{2+}$  from the cytosol equally efficiently at low ( $1 \text{ min}^{-1}$ ) and high ( $10 \text{ min}^{-1}$ ) bursting rates (Fig. 5b). Thus, the summation of  $[\text{Ca}^{2+}]_{\text{mit}}$  increases could not be explained by local effects of the non-sequestered cytosolic  $\text{Ca}^{2+}$ .

We next attempted to explore the potential contribution of ER  $\text{Ca}^{2+}$  uptake and release in sculpting the relationship between  $[\text{Ca}^{2+}]_{\text{cyt}}$  and  $[\text{Ca}^{2+}]_{\text{mit}}$ . To this end, we tested the effects of the sarco-(endo)plasmic reticulum  $\text{Ca}^{2+}$ -ATPase inhibitor cyclopiazonic acid (CPA). As expected,  $10 \mu\text{M}$  CPA abolished apparent  $\text{Ca}^{2+}$  accumulation into the ER (Fig. S4A) whereas a similar frequency dependence of  $[\text{Ca}^{2+}]_{\text{mit}}$  on  $[\text{Ca}^{2+}]_{\text{cyt}}$  pulses was observed as in the absence of the inhibitor (Fig. S4B vs. Fig. 3b). However, the use of this inhibitor was complicated by the fact that larger increases in  $[\text{Ca}^{2+}]_{\text{cyt}}$  were observed at each pulse, reflecting the functional loss of this important intracellular store (Fig. S4B).

Interestingly, activation of  $\text{Ca}^{2+}$  influx across the plasma membrane increased  $[\text{Ca}^{2+}]_{\text{mit}}$  more efficiently than the mobilisation of intracellular calcium (Fig. S5), in line with previous results [48]. Thus, when the former was activated by exposure to stepped pulses in extracellular  $\text{K}^{+}$  concentration, or the latter by exposure to varying acetyl choline concentrations (Fig. S5A), then for a given increase in  $[\text{Ca}^{2+}]_{\text{cyt}}$ , the increase in  $[\text{Ca}^{2+}]_{\text{mit}}$  was larger after the activation of  $\text{Ca}^{2+}$  influx from the extracellular space (Fig. S5B).

Cytosolic ATP/ADP increases are controlled by electrical bursting and  $[\text{Ca}^{2+}]_{\text{cyt}}$  oscillation frequency

We sought next to explore the functional consequences of the above relationship between  $[\text{Ca}^{2+}]_{\text{cyt}}$  and  $[\text{Ca}^{2+}]_{\text{mit}}$

**Fig. 3** The amplitude of  $[Ca^{2+}]_{mit}$  increases is regulated by the frequency of electrical bursts. **a** Epifluorescent images of the cell analysed in **B** with the ROI indicated (*red*) and pseudo-colour pixel-to-pixel ratios measured at four sequential time points. **b** Simultaneous recording of  $[Ca^{2+}]_{cyt}$  (*red*),  $[Ca^{2+}]_{mit}$  (*blue*) and  $V_m$  (*upper trace, black*). The cell was bathed in EC containing 16.7 mM glucose, with  $V_m$  being held at  $-70$  mV. The depolarisations were then imposed using the voltage clamp, with different rates being applied in random order. The arrows (*i–iv*) indicate the time points corresponding to the cell images in Fig. 3a. **c** Effect of the bursting frequency on the  $[Ca^{2+}]_{cyt}$  (*solid red*) and  $[Ca^{2+}]_{mit}$  (*solid blue*),  $n=13$ . Maximal values of  $[Ca^{2+}]_{cyt}$  and  $[Ca^{2+}]_{mit}$  of each five-burst train were normalised to the maximal values of the trains with maximal frequency ( $10\text{ min}^{-1}$ ), measured in the same cell. The  $[Ca^{2+}]_{cyt}$  and  $[Ca^{2+}]_{mit}$  data points that correspond to naturally occurring electrical activity (at 16.7 mM glucose, measured in the current clamp on the same cell) are given as *open red* ( $n=7$ ) and *open blue* ( $n=7$ ) squares, respectively. The differences between the neighbour points of  $[Ca^{2+}]_{mit}$  curve are statistically significant ( $P<0.02$ )

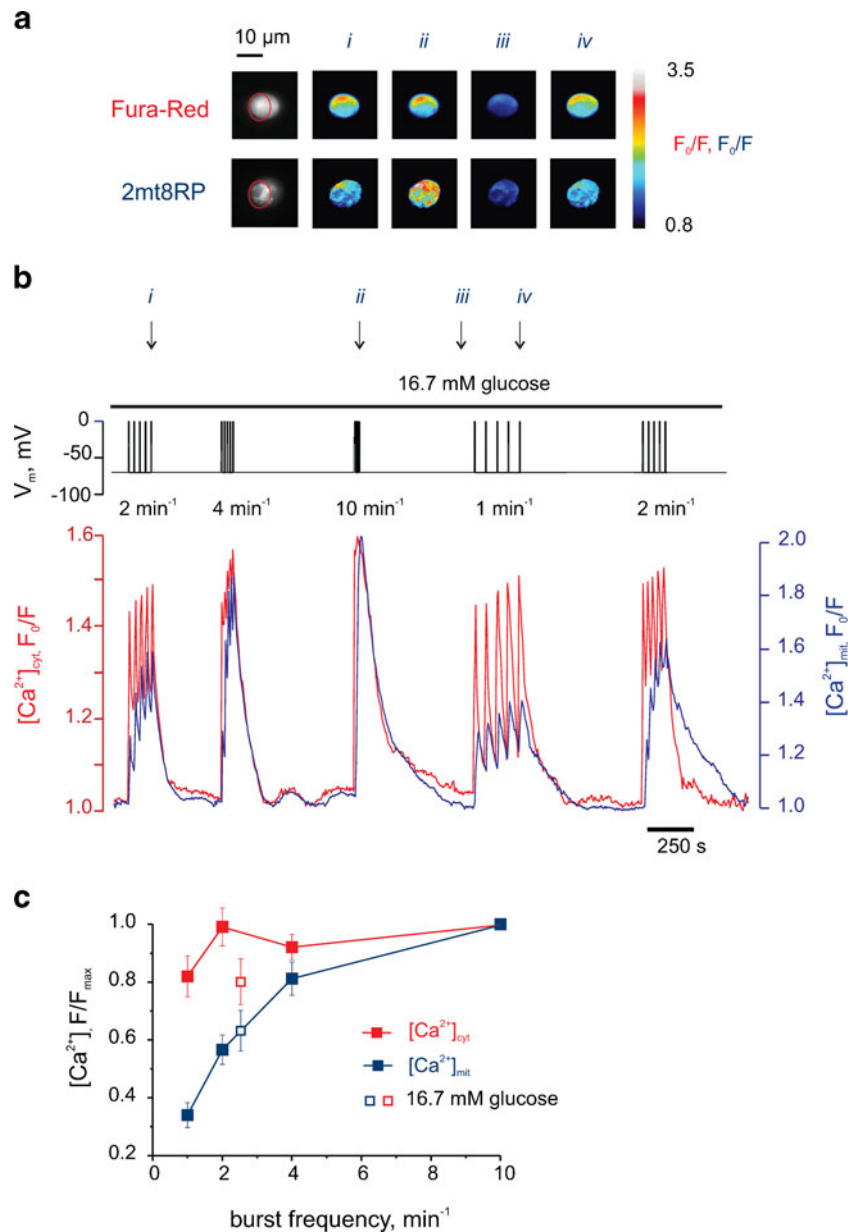


(Fig. 3b, c) by monitoring the cytosolic ATP/ADP ratio ( $[ATP/ADP]_{cyt}$ ) in real time with the recombinant green fluorescent protein-based probe *perceval* [6]. Extending our recent observations [51], we observed that the imposition with the patch pipette of  $[Ca^{2+}]_{cyt}$  oscillations at low frequency ( $1.0\text{ min}^{-1}$ ) had no discernible effect on the basal  $[ATP/ADP]_{cyt}$  (Fig. 6a), consistent with the small changes in  $[Ca^{2+}]_{mit}$  which occur during this protocol (Fig. 3b, c). By contrast, increasing the frequency of bursts to  $4\text{ min}^{-1}$  caused first a transient decrease in  $[ATP/ADP]_{cyt}$  and then a progressive increase in this ratio which, remarkably, continued after the termination of the pulses. Thus, the maximal amplitude of the  $[ATP/ADP]_{cyt}$  increases induced by bursts imposed at  $4\text{ min}^{-1}$  was  $2.8\pm 1.2$  times higher than that induced by a pulse rate of  $1\text{ min}^{-1}$  (Fig. 6b).

## Discussion

The principal aims of the present study were to assess the role and regulation of mitochondrial  $Ca^{2+}$  uptake and ATP synthesis during physiological (i.e. pulsatile) changes in cytosolic  $Ca^{2+}$ . To this end, we deployed our recently developed system [51] for imaging multiple parameters simultaneously in single cells, using the patch pipette to record or non-invasively manipulate plasma membrane potential and hence cytosolic  $Ca^{2+}$  with high precision. This approach, involving the use of a dispersed islet preparation, mimics many aspects of electrical and cytosolic  $Ca^{2+}$  oscillations observed for cells in situ within intact islets [49]. Although local interactions between small numbers of  $\beta$  cells within a cluster are retained, the preparation may not, however, fully

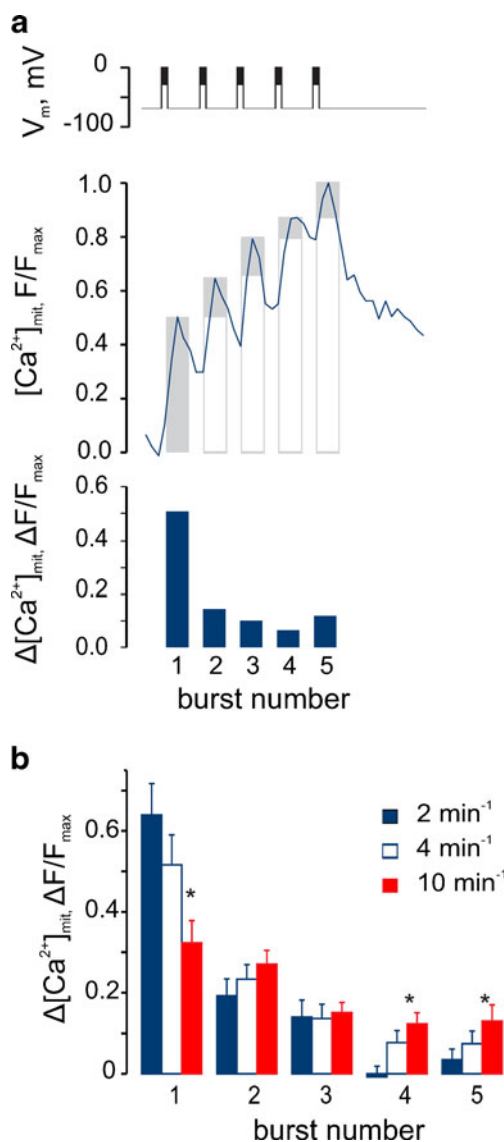


**Fig. 4** Summation of mitochondrial  $Ca^{2+}$  depends on the bursting frequency. **a** Determination of the differential contribution of each burst ( $\Delta[Ca^{2+}]_{mit(n)}$ ) for a 2-min<sup>-1</sup> train. *Upper graph*: the columns present maximal  $[Ca^{2+}]_{mit}$  within the burst normalized to maximal  $[Ca^{2+}]_{mit}$  within the whole five-burst train ( $[Ca^{2+}]_{mit(n)}/[Ca^{2+}]_{mit(max)}$ ). *Lower graph*: differential contribution of each burst ( $\Delta[Ca^{2+}]_{mit(n)}$ ). The columns represent the differences between each column and the preceding one, in the upper graph. **b** The differential contribution of each burst at different bursting frequencies. \* $P < 0.05$ , differences between the data at 2 and 10 min<sup>-1</sup> are statistically significant

replicate the collective effects of interactions across large number of  $\beta$  cells in the whole islet. Nevertheless, for studies of the sort undertaken here, this preparation provides marked advantages. Firstly, the expression of genes can be readily achieved and manipulated by viral gene (or shRNA) delivery, whereas the poor penetration of viral particles into the intact islet [14] limits the use of the latter for such studies. Secondly, during imaging, interference with signals from the recombinant FRET probes by endogenous autofluorescence is markedly reduced

compared to intact islets [41] (not shown). Lastly, the use of individual cells and clusters greatly facilitates the manipulation of the membrane potential through the patch pipette.

We show that silencing of *ccdc109a* (MCU) [5, 11], recently suggested to mediate  $Ca^{2+}$  entry into mitochondria as a complex with the regulator subunit MICU1 [36], inhibits glucose-induced insulin secretion to a small extent, whilst essentially eliminating secretion stimulated by tolbutamide (Fig. 1a–c). Since the effects of sulphonylureas are mediated by the elevation of the frequency of electrical spiking [17], we went on to examine in detail how individual electrical spikes are decoded by  $\beta$  cell mitochondria. We found that, under physiological conditions, changes in  $[Ca^{2+}]_{mit}$  in  $\beta$  cells are governed by the frequency of electrical bursting. Together with our earlier findings [1, 38, 51], our present results indicate the existence of a causal link between electrical activity and  $Ca^{2+}$ -mediated increases in mitochondrial ATP production.

We would stress that here, and in our earlier studies [40, 53], precise calibration of  $[Ca^{2+}]$  signals could not routinely be achieved. Nonetheless, post-experiment treatment with ionomycin, in high  $Ca^{2+}$ -containing solutions, was used to determine whether the probes were likely to have reached saturation. From these trials, and previous calibration of the mitochondrially targeted probe [19], which has indicated a  $K_d$  value of 1  $\mu$ M in situ, we estimate that maximal  $[Ca^{2+}]_{mit}$  levels extended into the low micromolar range at during peaks [47], exceeding those of  $[Ca^{2+}]_{cyt}$  ( $< 1 \mu$ M).

#### Role of mitochondrial $Ca^{2+}$ transport mediated by MCU in the control of insulin secretion

We have recently shown that silencing of the mitochondrial uniporter MCU has no detectable effect on the first phase (within  $\sim 5$  min) of glucose-induced electrical activity or ATP increase [51] whereas the second phase of glucose-induced ATP/ADP increase was sharply reduced. In the present study, we report that silencing of MCU leads to a modest inhibition of glucose-induced secretion of insulin, assayed with single-cell resolution by measuring the release of  $Zn^{2+}$  with the membrane-bound probe ZIMIR [26]. However, the further stimulation of insulin exocytosis by sulphonylureas was almost completely abolished.

The use of ZIMIR [26] in the present studies allowed a convenient means to study insulin secretion at the level of single cells and thus comparison with our subsequent measurements of  $Ca^{2+}$  and ATP dynamics in this preparation. However, this approach requires the continuous chelation of the secreted  $Zn^{2+}$ . The probe therefore allows a semi-quantitative assessment of the rate of insulin release, but is not optimal for dissecting the contributions of the first and second phases of secretion. Nonetheless, we were able to demonstrate effects on both glucose- and tolbutamide-stimulated secretion with this tool. Strikingly, the effects of



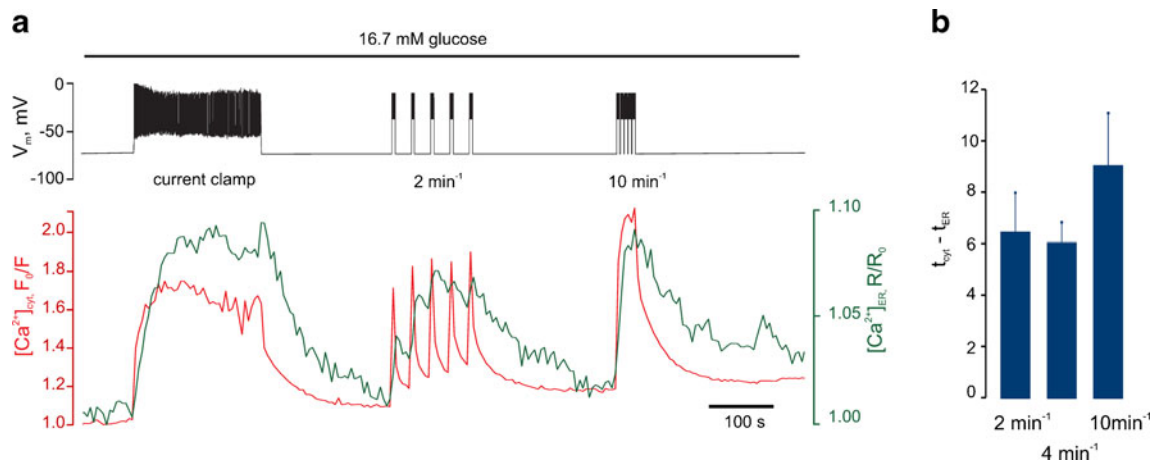


**Fig. 5** Effect of electrical bursting frequency on the apparent sequestration of  $Ca^{2+}$  by the ER. **a** Depolarisation-induced dynamics of  $[Ca^{2+}]_{ER}$ , data are a representative of  $n=6$  traces. The cell was bathed in the EC solution containing 16.7 mM glucose at 37 °C and  $[Ca^{2+}]_{ER}$  (green trace),  $[Ca^{2+}]_{cyt}$  (red trace) and  $V_m$  (upper trace) were monitored/manipulated simultaneously. The cell was held at  $V_m=-70$  mV initially, then the voltage clamp was released, as indicated by “current clamp” label on

the  $V_m$  trace and action potential spiking was observed. The cell was next re-clamped at  $-70$  mV, and after  $[Ca^{2+}]_{cyt}$  and  $[Ca^{2+}]_{ER}$  had reached the basal levels, the depolarisation protocol (Suppl. Fig. S1) was applied at the frequency of 4 and 10 min<sup>-1</sup>, as indicated. **b** The delay between maximal increase in  $[Ca^{2+}]_{cyt}$  and  $[Ca^{2+}]_{ER}$  in response to five depolarizing trains applied at 2, 4 and 10 min<sup>-1</sup>

tolbutamide were markedly (by >80 %) diminished in MCU-silenced cells (Fig. 1a, c). We suspect that this may reflect diminished secretory granule competence (or translocation towards release sites), perhaps as a result of impaired mitochondrial ATP synthesis. In support of this view, our earlier studies [53] revealed a marked decrease in the second phase of glucose-induced ATP increase in MCU-silenced vs. scrambled shRNA-treated cells. Thus, at the time point of addition of tolbutamide in the experiments performed here ( $\geq 600$  s after the addition of high glucose; Fig. 1), the cytosolic ATP/ADP ratio in MCU-silenced cells is expected to be significantly lower than in control cells.

A recent report has shown that MCU silencing impairs insulin secretion stimulated from clonal rat insulinoma cells, INS-1(832/13), by 16 mM glucose [3]. Although clonal  $\beta$  cells display a number of metabolic and secretory abnormalities (see [50]), a  $\sim 50$  % decrease in insulin secreted within 1 h [3] agrees well with the idea that the second phase of insulin secretion relies upon mitochondrial  $Ca^{2+}$  entry. This interpretation is, furthermore, consistent with the selective impairment of the second phase of glucose-stimulated insulin secretion from rat islets in which mitochondrial  $Ca^{2+}$  increases were buffered with the  $Ca^{2+}$  binding protein, S100G [55].

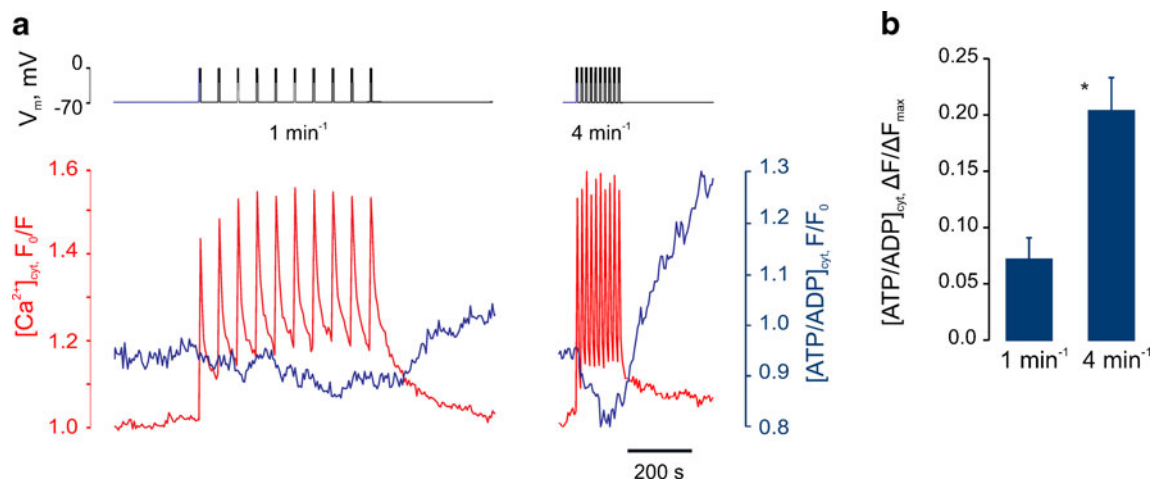


**Fig. 6** Electrical bursting frequency controls cytosolic ATP/ADP increases. **a**  $\beta$  Cells were voltage-clamped at  $-70$  mV at 16.7 mM glucose and 10-burst trains of depolarisations were imposed at 1 or 4 min<sup>-1</sup>.  $[ATP/ADP]_{cyt}$  and  $[Ca^{2+}]_{cyt}$  were reported by Perceval and Fura-Red, respectively. **b** Mean  $[ATP/ADP]_{cyt}$  potentiation in response

to depolarisation at 1 min<sup>-1</sup> ( $n=14$ ) or 4 min<sup>-1</sup> ( $n=16$ ). The data were normalised to the width of the range of  $[ATP/ADP]_{cyt}$  change between application of 16.7 mM glucose and 2  $\mu$ M FCCP ( $\Delta F_{max}$ ). \* $P<0.01$ , differences are significant

## Frequency control of mitochondrial $\text{Ca}^{2+}$ accumulation and ATP synthesis

Given the importance of mitochondrial  $\text{Ca}^{2+}$  uptake for the normal stimulation of insulin secretion demonstrated in the present and previous [3, 55] studies, it seemed important to understand whether and how the subtle fine tuning of cytosolic  $\text{Ca}^{2+}$  concentration by glucose and other secretagogues, including variations in oscillation frequency, regulates mitochondrial free  $[\text{Ca}^{2+}]$  and consequently cytosolic ATP/ADP. Consistent with our recent findings [53], we show that in response to an elevation of glucose concentration from 3 to 16.7 mM, a progressive increase in  $[\text{Ca}^{2+}]_{\text{mit}}$  occurs in the dissociated mouse  $\beta$  cells (Fig. 2a). This increase, which clearly lagged behind the increase in  $[\text{Ca}^{2+}]_{\text{cyt}}$ , was somewhat slower in onset and more stable than increases reported in dispersed rat islets by Wiederkehr and colleagues [55]. Importantly,  $[\text{Ca}^{2+}]_{\text{mit}}$  remained elevated whilst  $[\text{Ca}^{2+}]_{\text{cyt}}$  remained at the peak in the same cells. Furthermore, the application of high extracellular  $[\text{K}^+]$  to depolarise the membrane [55] has been shown to stimulate the activity of plasma membrane  $\text{Na}^+-\text{K}^+$  ATPase and hence alter both cellular energetic and ion homeostasis [56]. We note that parallel measurements of  $[\text{Ca}^{2+}]$  in each compartment were also not possible in the earlier study [55] where a mitochondrially targeted aequorin was used to measure  $[\text{Ca}^{2+}]_{\text{mit}}$  through bioluminescence recordings.

Using the more sensitive, fluorescence-based, probe for mitochondrial  $\text{Ca}^{2+}$ , 2mt8RP [18] in single primary  $\beta$  cells, we show firstly that brief  $[\text{Ca}^{2+}]_{\text{cyt}}$  spikes following a single (or a small number of) action potentials barely affect  $[\text{Ca}^{2+}]_{\text{mit}}$  (Fig. 2a). However, the limited increases in mitochondrial  $\text{Ca}^{2+}$  that do occur under these conditions appeared to reverse slowly, such that a slow but progressive increase in  $[\text{Ca}^{2+}]_{\text{mit}}$  could be observed. This integration or “summation” of the cytosolic  $\text{Ca}^{2+}$  peaks led us to explore the possibility that their frequency may control the eventual amplitude of the  $[\text{Ca}^{2+}]_{\text{mit}}$  increases. By imposing such pulsatile changes in cytosolic  $\text{Ca}^{2+}$  through the manipulation of the membrane potential of single cells (Figs. 3 and 4), we provide evidence for such a model.

Thus, we show that  $\beta$  cell mitochondria achieve decoding of “frequency-tuned” cytosolic signals. What may be the physiological significance of this relationship? Firstly, we suspect that it provides a mechanism to ensure that the energetic demands of increased electrical activity are matched by elevated ATP synthesis, hence preventing the termination of the glucose signal (due to the re-opening of  $\text{K}_{\text{ATP}}$  channels). Secondly, it may mitigate the longer-term effects of supraphysiological stimulation, e.g. with sulphonylureas, a process akin to the excitotoxicity which leads to excessive  $\text{Ca}^{2+}$  influx and eventual cell death in neurons [27]. Thirdly, a positive feedback effect of enhanced electrical activity to increase ATP production may conceivably contribute to the steep, “switch-like” dose response of insulin secretion to glucose [31]. However, the

activation of mitochondrial ATP synthesis by  $\text{Ca}^{2+}$  is likely to saturate and reverse above a certain limit (due to excessive  $\text{Ca}^{2+}$  accumulation, mitochondrial uncoupling and possibly the opening of permeability transition pores) [22]. The cell will then “reset” (thanks to the reopening of  $\text{K}_{\text{ATP}}$  and other channels) to a lower level of electrical and secretory activity.

Earlier evidence for the regulation of mitochondrial oxidative metabolism by cytosolic  $\text{Ca}^{2+}$  oscillations was obtained some years ago in hepatocytes [21], where mitochondrial pyridine nucleotide (NAD(P)H) fluorescence was assessed in response to vasopressin or other inositol 1,4,5-*tris*phosphate ( $\text{IP}_3$ )-generating hormones. However, measurements of intramitochondrial  $\text{Ca}^{2+}$  were not performed in the previous study. Likewise, Pralong and colleagues [39] were also able to demonstrate in a variety of cell types (rat pancreatic  $\beta$ -, adrenal glomerulosa and liver) that oscillations in  $[\text{Ca}^{2+}]_{\text{cyt}}$  were closely tracked by those in NAD(P)H fluorescence when the frequency of  $[\text{Ca}^{2+}]_{\text{cyt}}$  oscillations remained low (for example, in  $\beta$  cells, at 8.3 mM glucose). By contrast, high-frequency cytosolic  $\text{Ca}^{2+}$  oscillations (e.g. at 11.2 mM glucose for  $\beta$  cells) induced the confluence of the individual NAD(P)H spikes and a stable elevation of this parameter. These earlier, and the present study, thus support the view that frequency of oscillations in cytosolic  $\text{Ca}^{2+}$  regulates the amplitude of the changes in fuel metabolism by mitochondria, adding to the list of cellular processes, such as gene expression in immune cells [16], which are controlled in this way. Such “demodulation” may therefore represent a common mechanism for the decoding by intracellular organelles of cytosolic  $\text{Ca}^{2+}$  signals, which avoids the potentially damaging consequences of more stable increases in  $[\text{Ca}^{2+}]_{\text{cyt}}$ .

### Roles for “mitochondrial plasticity” in the $\beta$ cell?

An interesting observation made during the course of the present studies was the absence of any evident “desensitisation” of mitochondrial  $\text{Ca}^{2+}$  increases during repeated cytosolic  $\text{Ca}^{2+}$  pulses (Figs. S2 and 3), in contrast to previous findings in primary rat  $\beta$ - and insulinoma-derived INS1 cells [29] where a “run-down” in the increases was observed. Whether this reflects a difference in the behaviour of rat vs. mouse  $\beta$  cells, or the use of large populations of cells in the earlier study (where the behaviour of a cell sub-population may have biased recordings using aequorin), is presently unclear. On the other hand, and in contrast to the findings of Csordas and Hajnoczky in a mast cell line [9], we observed no increase in the amplitude of the successive  $[\text{Ca}^{2+}]_{\text{mit}}$  increases when  $V_{\text{m}}/[\text{Ca}^{2+}]_{\text{cyt}}$  spikes were sufficiently well-spaced (e.g. at  $0.5 \text{ min}^{-1}$ ; Fig. S2) that an opportunity for mitochondrial  $\text{Ca}^{2+}$  accumulation between  $[\text{Ca}^{2+}]_{\text{cyt}}$  peaks did not exist. Thus,  $\text{Ca}^{2+}$ -dependent re-configuration of ER-mitochondria contacts (“mitochondrial plasticity”) [46] appears not to be involved in regulating  $\text{Ca}^{2+}$  influx into  $\beta$  cell mitochondria.

By contrast, we provide further evidence (Fig. 6) that an alternative form of mitochondrial plasticity, described in earlier studies [1, 24], plays a role in shaping the metabolic responses of the  $\beta$  cell to glucose. Thus, after an initial drop, presumably reflecting increased cytosolic ATP consumption (e.g. for ion pumping), a steady and ultimately quite dramatic rise in ATP/ADP was observed, likely reflecting the stimulation of the intramitochondrial dehydrogenases and components of the respiratory chain [10].

Finally, the present studies also demonstrate that changes in ER  $\text{Ca}^{2+}$  are more sensitive to  $[\text{Ca}^{2+}]_{\text{cyt}}$  increases than those in the mitochondria (Fig. 5). Thus, it appears that these two organellar systems (ER vs. mitochondria) may be able, at least in the  $\beta$  cell, to sense and decode  $[\text{Ca}^{2+}]_{\text{cyt}}$  oscillations differently, a reflection of the distinct  $\text{Ca}^{2+}$  transporting machinery with which each is equipped. The consequences for ER function, notably protein synthesis, and for ER stress, are presently unclear.

## Conclusions

Extending our earlier findings [51, 53], we demonstrate here that (1) mitochondrial  $\text{Ca}^{2+}$  accumulation, mediated by MCU, is an important determinant of tolbutamide- and to a lesser extent glucose-stimulated insulin secretion from primary  $\beta$  cells and (2) that mitochondria in these cells integrate cytosolic pulses to modulate  $[\text{Ca}^{2+}]_{\text{mit}}$  changes and ATP synthesis. Given the impairment in the normal pulsatility in insulin secretion observed in type 2 diabetes [34], it is conceivable that a derangement in the generation of cytosolic  $\text{Ca}^{2+}$  oscillations may even be a primary event which contributes to downstream production of ATP and hence insulin secretion. Whether pharmacological modulation of mitochondrial  $\text{Ca}^{2+}$  uptake may, therefore, regulate insulin secretion in vivo, and might thus provide a new approach to improve glucose tolerance in some forms of diabetes mellitus, is an intriguing question for the future.

**Acknowledgments** The study was supported by the Wellcome Trust (programme grant 081958/Z/07/Z and Senior Investigator Award WT098424A1A) and a Royal Society Wolfson Research Merit Award to G.A.R. AIT received a Juvenile Diabetes Research Foundation (JDRF) Postdoctoral Fellowship and Daliang Li a JDRF grant (37-2011-21). PG is Research Director of the Fonds National de la Recherche Scientifique, Brussels. MAR is Chargé de Recherches from INSERM, Paris. RR thanks Telethon-Italy, Italian Association for Cancer Research, the Italian Ministry of Education (PRIN, FIRB), the Cariparo Foundation and the European Research Council (“mitoCalcium”). We are grateful to Profs. G Yellen (Yale), R.M Denton, P.J. Cullen (University of Bristol) and Dr W-H.Li (UT South Western) for useful discussion.

**Open Access** This article is distributed under the terms of the Creative Commons Attribution License which permits any use, distribution, and reproduction in any medium, provided the original author(s) and the source are credited.

## References

1. Ainscow EK, Rutter GA (2001) Mitochondrial priming modifies  $\text{Ca}^{2+}$  oscillations and insulin secretion in pancreatic islets. *Biochem J* 353:175–180
2. Ainscow EK, Rutter GA (2002) Glucose-stimulated oscillations in free cytosolic ATP concentration imaged in single islet  $\beta$  cells: evidence for a  $\text{Ca}^{2+}$ -dependent mechanism. *Diabetes* 51:S162–S170
3. Alam MR, Groschner LN, Parichatikanond W, Kuo L, Bondarenko AI, Rost R, Waldeck-Weiermair M, Malli R and Graier WF (2012) Mitochondrial  $\text{Ca}^{2+}$  uptake 1 (MICU1) and mitochondrial  $\text{Ca}^{2+}$  uniporter (MCU) contribute to metabolism-secretion coupling in clonal pancreatic beta-cells. *J Biol Chem* 287:34445–34454
4. Ashcroft SJH (2000) The beta-cell K-ATP channel. *J Membrane Biol* 176:187–206
5. Baughman JM, Perocchi F, Girgis HS, Plovanich M, Belcher-Timme CA, Sancak Y, Bao XR, Strittmatter L, Goldberger O, Bogorad RL, Kotliansky V et al (2011) Integrative genomics identifies MCU as an essential component of the mitochondrial calcium uniporter. *Nature* 476:341–345
6. Berg J, Hung YP, Yellen G (2009) A genetically encoded fluorescent reporter of ATP:ADP ratio. *Nat Methods* 6:161–166
7. Berridge MJ, Lipp P, Bootman MD (2000) The versatility and universality of calcium signalling. *Nat Rev Mol Cell Biol* 1:11–21
8. Corkey BE, Tornheim K, Deeney JT, Glennon MC, Parker JC, Matschinsky FM, Ruderman NB, Prentki M (1988) Linked oscillations of free  $\text{Ca}^{2+}$  and the ATP/ADP ratio in permeabilized RINm5F insulinoma cells supplemented with a glycolyzing cell-free muscle extract. *J Biol Chem* 263:4254–4258
9. Csordas G, Hajnoczky G (2003) Plasticity of mitochondrial calcium signaling. *J Biol Chem* 278:42273–42282
10. Davidson AM, Halestrap AP (1989) Inhibition of mitochondrial-matrix inorganic pyrophosphatase by physiological ( $\text{Ca}^{2+}$ ), and its role in the hormonal regulation of mitochondrial matrix volume. *Biochem J* 258:817–821
11. De Stefani D, Raffaello A, Teardo E, Szabo I, Rizzuto R (2011) A forty-kilodalton protein of the inner membrane is the mitochondrial calcium uniporter. *Nature* 476:336–340
12. Denton RM, McCormack JG (1980) On the role of the calcium transport cycle in the heart and other mammalian mitochondria. *FEBS Lett* 119:1–8
13. Detimary P, Gilon P, Henquin JC (1998) Interplay between cytoplasmic  $\text{Ca}^{2+}$  and the ATP/ADP ratio: a feedback control mechanism in mouse pancreatic islets. *Biochem J* 333:269–274
14. Diraison F, Parton L, Ferre P, Fougelle F, Briscoe CP, Leclerc I, Rutter GA (2004) Over-expression of sterol-regulatory-element-binding protein-1c (SREBP1c) in rat pancreatic islets induces lipogenesis and decreases glucose-stimulated insulin release: modulation by 5-aminoimidazole-4-carboxamide ribonucleoside (AICAR). *Biochem J* 378:769–778
15. Dolmetsch RE, Lewis RS, Goodnow CC, Healy JI (1997) Differential activation of transcription factors induced by  $\text{Ca}^{2+}$  response amplitude and duration. *Nature* 386:855–858
16. Dolmetsch RE, Xu KL, Lewis RS (1998) Calcium oscillations increase the efficiency and specificity of gene expression. *Nature* 392:933–936
17. Ferrer R, Atwater I, Omer EM, Goncalves AA, Croghan PC, Rojas E (1984) Electrophysiological evidence for the inhibition of

- potassium permeability in pancreatic beta-cells by glibenclamide. *Q J Exp Physiol* 69:831–839
18. Filippin L, Abad MC, Gastaldello S, Magalhaes PJ, Sandona D, Pozzan T (2005) Improved strategies for the delivery of GFP-based Ca<sup>2+</sup> sensors into the mitochondrial matrix. *Cell Calcium* 37:129–136
  19. Filippin L, Magalhaes PJ, Di Benedetto G, Colella M, Pozzan T (2003) Stable interactions between mitochondria and endoplasmic reticulum allow rapid accumulation of calcium in a subpopulation of mitochondria. *J Biol Chem* 278:39224–39234
  20. Gopel SO, Kanno T, Barg S, Eliasson L, Galvanovskis J, Renstrom E, Rorsman P (1999) Activation of Ca(2+)-dependent K(+) channels contributes to rhythmic firing of action potentials in mouse pancreatic beta cells. *J Gen Physiol* 114:759–770
  21. Hajnoczky G, Robb-Gaspers LD, Seitz MB, Thomas AP (1995) Decoding of cytosolic calcium oscillations in the mitochondria. *Cell* 82:415–424
  22. Halestrap AP (2010) A pore way to die: the role of mitochondria in reperfusion injury and cardioprotection. *Biochem Soc Trans* 38:841–860
  23. Henquin JC (2009) Regulation of insulin secretion: a matter of phase control and amplitude modulation. *Diabetologia* 52:739–751
  24. Jouaville LS, Pinton P, Bastianutto C, Rutter GA and Rizzuto R (1999) Regulation of mitochondrial ATP synthesis by calcium: evidence for a long-term metabolic priming. *Proc Natl Acad Sci U S A* 96:13807–13812
  25. Kennedy ED, Rizzuto R, Theler JM, Pralong WF, Bastianutto C, Pozzan T, Wollheim CB (1996) Glucose-stimulated insulin secretion correlates with changes in mitochondrial and cytosolic Ca<sup>2+</sup> in aequorin-expressing INS-1 cells. *J Clin Invest* 98:2524–2538
  26. Li D, Chen S, Bellomo EA, Tarasov AI, Kaut C, Rutter GA, Li WH (2011) Imaging dynamic insulin release using a fluorescent zinc probe, ZIMIR. *Proc Natl Acad Sci U S A* 108:21063–21068
  27. Lipton SA, Rosenberg PA (1994) Excitatory amino acids as a final common pathway for neurologic disorders. *N Engl J Med* 330:613–622
  28. Luo J, Deng ZL, Luo X, Tang N, Song WX, Chen J, Sharff KA, Luu HH, Haydon RC, Kinzler KW, Vogelstein B et al (2007) A protocol for rapid generation of recombinant adenoviruses using the AdEasy system. *Nat Protoc* 2:1236–1247
  29. Maechler P, Kennedy ED, Wang HY, Wollheim CB (1998) Desensitization of mitochondrial Ca<sup>2+</sup> and insulin secretion responses in the beta cell. *J Biol Chem* 273:20770–20778
  30. Maechler P, Wollheim CB (2001) Mitochondrial function in normal and diabetic beta-cells. *Nature* 414:807–812
  31. Malaisse WJ, Sener JA, Herchuelz A, Hutton JC (1979) Insulin release: the fuel hypothesis. *Metabolism* 28:373–385
  32. Manning Fox JE, Gyulkhandanyan AV, Satin LS, Wheeler MB (2006) Oscillatory membrane potential response to glucose in islet beta-cells: a comparison of islet-cell electrical activity in mouse and rat. *Endocrinology* 147:4655–4663
  33. Meissner HP (1990) Membrane potential measurements in pancreatic beta cells with intracellular microelectrodes. *Methods Enzymol* 192:235–246
  34. O'Rahilly S, Turner RC, Matthews DR (1988) Impaired pulsatile secretion of insulin in relatives of patients with non-insulin-dependent diabetes. *N Engl J Med* 318:1225–1230
  35. Palmer AE, Jin C, Reed JC, Tsien RY (2004) Bcl-2-mediated alterations in endoplasmic reticulum Ca<sup>2+</sup> analyzed with an improved genetically encoded fluorescent sensor. *Proc Natl Acad Sci U S A* 101:17404–17409
  36. Perocchi F, Gohil VM, Girgis HS, Bao XR, McCombs JE, Palmer AE, Mootha VK (2010) MICU1 encodes a mitochondrial EF hand protein required for Ca(2+) uptake. *Nature* 467:291–296
  37. Pinton P, Giorgi C, Siviero R, Zecchini E, Rizzuto R (2008) Calcium and apoptosis: ER-mitochondria Ca<sup>2+</sup> transfer in the control of apoptosis. *Oncogene* 27:6407–6418
  38. Pralong WF, Bartley C, Wollheim CB (1990) Single islet beta-cell stimulation by nutrients: relationship between pyridine nucleotides, cytosolic Ca<sup>2+</sup> and secretion. *EMBO J* 9:53–60
  39. Pralong WF, Spat A, Wollheim CB (1994) Dynamic pacing of cell metabolism by intercellular Ca<sup>2+</sup> transients. *J Biol Chem* 269:27310–27314
  40. Ravier MA, Daro D, Roma LP, Jonas JC, Cheng-Xue R, Schuit FC, Gilon P (2011) Mechanisms of control of the free Ca<sup>2+</sup> concentration in the endoplasmic reticulum of mouse pancreatic {beta}-cells: interplay with cell metabolism and [Ca<sup>2+</sup>]<sub>c</sub>, and role of SERCA2b and SERCA3. *Diabetes* 60:2533–2545
  41. Ravier MA, Rutter GA (2005) Glucose or insulin, but not zinc ions, inhibit glucagon secretion from mouse pancreatic alpha-cells. *Diabetes* 54:1789–1797
  42. Rutter GA (1990) Ca<sup>2+</sup>-binding to citrate cycle enzymes. *Int J Biochem* 22:1081–1088
  43. Rutter GA (2001) Nutrient-secretion coupling in the pancreatic islet β-cell: recent advances. *Molecular Aspects of Medicine* 22:247–284
  44. Rutter GA (2004) Visualising insulin secretion. The Minkowski lecture 2004. *Diabetologia* 47:1861–1872
  45. Rutter GA, Pralong W-F, Wollheim CB (1992) Regulation of mitochondrial glycerol phosphate dehydrogenase activity by Ca<sup>2+</sup> within electroporabilized insulin-secreting cells (INS1). *Biochimica et Biophysica Acta - Bioenergetics* 1175:107–113
  46. Rutter GA, Rizzuto R (2000) Regulation of mitochondrial metabolism by ER Ca<sup>2+</sup> release: an intimate connection. *Trends Biochem Sci* 25:215–221
  47. Rutter GA, Theler J-M, Murta M, Wollheim CB, Pozzan T, Rizzuto R (1993) Stimulated Ca<sup>2+</sup> influx raises mitochondrial free Ca<sup>2+</sup> to supramicromolar levels in a pancreatic β-cell line: possible role in glucose and agonist-induced insulin secretion. *J Biol Chem* 268:22385–22390
  48. Rutter GA, Tsuboi T, Ravier MA (2006) Ca<sup>2+</sup> microdomains and the control of insulin secretion. *Cell Calcium* 40:539–551
  49. Santos RM, Rosario LM, Nadal A, Garcia-Sancho J, Soria B, Valdeolmillos M (1991) Widespread synchronous [Ca<sup>2+</sup>]<sub>i</sub> oscillations due to bursting electrical activity in single pancreatic islets. *Eur J Physiol* 418:417–422
  50. Sekine N, Cirulli V, Regazzi R, Brown LJ, Gine E, Tamarit-Rodriguez J, Girotti M, Marie S, MacDonald MJ, Wollheim CB, Rutter GA (1994) Low lactate dehydrogenase and high mitochondrial glycerol phosphate dehydrogenase in pancreatic β-cell. Potential role in nutrient sensing. *J Biol Chem* 269:4895–4902
  51. Tarasov AI, Griffiths EJ, Rutter GA (2012) Regulation of ATP production by mitochondrial Ca(2+). *Cell Calcium* 52:28–35
  52. Tarasov AI, Nicolson T, Riveline JP, Taneja TK, Baldwin SA, Baldwin JM, Charpentier G, Gautier JF, Froguel P, Vaxillaire M, Rutter GA (2008) A rare mutation in ABCC8/SUR1 leading to altered KATP channel activity and {beta}-cell glucose sensing is associated with type 2 diabetes mellitus in adults. *Diabetes* 57:1595–1604
  53. Tarasov AI, Ravier MA, Semplici F, Bellomo EA, Pullen TJ, Gilon P, Sekler I, Rizzuto R, Rutter GA (2012) The mitochondrial Ca<sup>2+</sup> uniporter MCU is essential for glucose-induced ATP increases in pancreatic beta-cells. *PLoS One* 7(7):e39722
  54. Whitaker M (2008) Calcium signalling in early embryos. *Philos Trans R Soc Lond B Biol Sci* 363:1401–1418
  55. Wiederkehr A, Szanda G, Akhmedov D, Matakic C, Heizmann CW, Schoonjans K, Pozzan T, Spat A, Wollheim CB (2011) Mitochondrial matrix calcium is an activating signal for hormone secretion. *Cell Metab* 13:601–611
  56. Yingst DR, Davis J, Schiebinger R (2001) Effects of extracellular calcium and potassium on the sodium pump of rat adrenal glomerulosa cells. *Am J Physiol Cell Physiol* 280:C119–C125